PROTEINS
STRUCTURE ■ FUNCTION ■ BIOINFORMATICS

Analysis of the electrochemistry of hemes with E_ms spanning 800 mV

Zhong Zheng and M. R. Gunner*

Department of Physics, The City College of New York, New York, New York

ABSTRACT

The free energy of heme reduction in different proteins is found to vary over more than 18 kcal/mol. It is a challenge to determine how proteins manage to achieve this enormous range of E_ms with a single type of redox cofactor. Proteins containing 141 unique hemes of *a*-, *b*-, and *c*-type, with bis-His, His-Met, and aquo-His ligation were calculated using Multi-Conformation Continuum Electrostatics (MCCE). The experimental E_ms range over 800 mV from −350 mV in cytochrome c_3 to 450 mV in cytochrome *c* peroxidase (vs. SHE). The quantitative analysis of the factors that modulate heme electrochemistry includes the interactions of the heme with its ligands, the solvent, the protein backbone, and sidechains. MCCE calculated E_ms are in good agreement with measured values. Using no free parameters the slope of the line comparing calculated and experimental E_ms is 0.73 (R^2 = 0.90), showing the method accounts for 73% of the observed E_m range. Adding a +160 mV correction to the His-Met c-type hemes yields a slope of 0.97 (R^2 = 0.93). With the correction 65% of the hemes have an absolute error smaller than 60 mV and 92% are within 120 mV. The overview of heme proteins with known structures and E_ms shows both the lowest and highest potential hemes are *c*-type, whereas the *b*-type hemes are found in the middle E_m range. In solution, bis-His ligation lowers the E_m by ≈205 mV relative to hemes with His-Met ligands. The bis-His, aquo-His, and His-Met ligated *b*-type hemes all cluster about E_ms which are ≈200 mV more positive in protein than in water. In contrast, the low potential bis-His *c*-type hemes are shifted little from in solution, whereas the high potential His-Met *c*-type hemes are raised by ≈300 mV from solution. The analysis shows that no single type of interaction can be identified as the most important in setting heme electrochemistry in proteins. For example, the loss of solvation (reaction field) energy, which raises the E_m, has been suggested to be a major factor in tuning *in situ* E_ms. However, the calculated solvation energy vs. experimental E_m shows a slope of 0.2 and R^2 of 0.5 thus correlates weakly with E_ms. All other individual interactions show even less correlation with E_m. However the sum of these terms does reproduce the range of observed E_ms. Therefore, different proteins use different aspects of their structures to modulate the *in situ* heme electrochemistry. This study also shows that the calculated E_ms are relatively insensitive to different heme partial charges and to the protein dielectric constant used in the simulation.

Proteins 2009; 75:719–734.

Key words: cytochrome; MCCE; E_m; continuum electrostatics; ligand; heme.

INTRODUCTION

A group of versatile and important proteins incorporate hemes as cofactors. In biological electron transfer chains, the cofactor midpoint redox potential controls the direction of favorable transport between the individual cofactors.[1,2] Thus, the *in situ* heme E_m determines the role the protein will play. These proteins carry out diverse biological functions. For example, *c* type cytochromes are responsible for electron transport in respiratory pathways.[3,4] Cytochromes P450 carry out substrate oxidation.[5] Heme proteins also play roles that do not involve redox reactions, in sensing, storing, and transporting small ligands,[6] metal ions,[7] and gases such as oxygen and carbon monoxide.[8,9] The release of cytochrome *c* from the mitochondria into the cytosol initiates programmed cell death.[10,11] In addition, heme has become a favored cofactor to be bound to *de novo* designed and bioinspired proteins to generate new functionality.[12–14]

Reported heme E_ms cover an enormous range of 1000 mV from −550 mV for His-Tyr *b* type heme in HasA[15] to 450 mV for His-Met *c* type heme in cytochrome *c* Peroxidase.[16,17] This represents a shift of 23.5 kcal/mol for the reduction reaction, equivalent to a protein changing the pK_a of a given residue type by 17.4 pH units. A

Additional Supporting Information may be found in the online version of this article.
Grant sponsor: NSF; Grant number: MCB-0517589; Grant sponsor: NIH; Grant number: 5G12 RR03060.
*Correspondence to: M. R. Gunner, Department of Physics, the City College of New York, New York, NY. E-mail: gunner@sci.ccny.cuny.edu
Received 17 June 2008; Revised 28 August 2008; Accepted 5 September 2008
Published online 29 September 2008 in Wiley InterScience (www.interscience.wiley.com). DOI: 10.1002/prot.22282

major challenge for understanding the relationship between protein structure and function is to identify the forces that proteins use to modify the behavior of bound ligands. The simplicity of the heme electrochemistry with its one electron oxidation/reduction reaction, the extreme range of modification of the chemistry *in situ* and the wealth of data and structures allows the in depth computational study of this group of proteins.

Cytochrome E_ms have been analyzed by various computational techniques to understand how the protein modifies the heme electrochemistry. Studies have used classical continuum electrostatics (CE),[18–21] MultiConformation Continuum Electrostatics (MCCE),[22] Protein Dipoles Langevin dipoles (PDLD), semi-microscopic PDLD (PDLD/S) analysis,[23,24] Molecular Dynamics (MD),[25] and QM and QM/MM[26] methods. Calculations on the *Rhodopseudomonas viridis* reaction center, which have four hemes with E_ms spanning 450 mV, successfully identified the high- and low-potential hemes.[18,27] Mao investigated a variety of soluble cytochromes with E_ms spanning 450 mV using MCCE, comparing the ways different protein folding motifs modulate the electrochemistry.[22] A variety of studies have shown the importance of the propionic acids, which are peripheral groups to the heme in determining the E_m and the pH dependence of the E_ms.[19,28,29]

Many of the methods that analyze heme E_ms in proteins are conceptually similar to those that calculate residue pK_as in proteins, analyzing how the protein shifts the proton affinity of a site.[30–35] However, proteins are found to shift heme E_ms over a much larger range than amino acid pK_as. Protein pK_as are usually measured from pH 2 to 11 where proteins remain stable.[30,36,37] Althougth the observed pK_as for a given residue type range over only a few pH units,[38,39] some highly perturbed species can be found where the protein shifts the pK_as by as much as 4–5 pH units.[40,41] This represents a shift in free energy of ionization of 240–300 meV, much smaller than found routinely for the shifts in heme E_ms.

The earliest analysis of heme protein electrochemistry focused on how the desolvation of the heme in the protein will raise the E_m relative to that found for a heme in water.[42–44] Modern continuum electrostatics techniques then combined continuum electrostatics energies and Monte Carlo sampling of the possible combinations of ionization states in a protein. This analysis starts with a reference $pK_{a,sol}$ or $E_{m,sol}$ in water for each group of interest calculating the shift in pK_a or E_m when the group is moved into the protein.[31] The free energy of the reaction is assumed to be shifted by the change in solvation energy and by electrostatic pairwise interactions with charges and dipoles between the water and protein, which are calculated by the Poisson-Boltzmann (PB) equation[45] or Generalized Born methods.[46,47] Monte Carlo sampling establishes the Boltzmann distribution of all acids and bases and redox active sites as a function of pH and E_h, yielding the calculated pK_as and E_ms within the protein. There have long been arguments about the most appropriate value for the protein dielectric constant. Different values have been tried, from as low as 4[36,48,49] to 8,[38] 20[20,50] and to as high as 80.[51] There have also been methods using nonuniform dielectric constants.[52,53] All these represent different levels of averaging the response to changes in charge. MCCE adds extensive rotamer sampling to the sampling of ionization states found in traditional continuum electrostatic calculations. This added degree of freedom raises the local effective dielectric response and improves the match between observed and calculated E_ms or pK_as.[22,36] MCCE has proven to be a good tool in calculating pK_as and E_ms of residues and cofactors in proteins.[22,28,54–57]

Earlier calculations on heme proteins analyzed either one protein[18,19,58] or several proteins covering a small range of E_ms.[20,22] The work reported here is the first using a single method to analyze proteins with hemes covering an E_m spread of 800 mV, almost twice as large as the 450 mV range previously explored.[22] Most bis-His, His-Met, and aquo-His ligated heme containing proteins with known E_ms as of March 2007 were analyzed. Using the standard continuum electrostatics analysis there are no free parameters in the E_m calculation as long as the appropriate E_m of the heme with the ligand in solution ($E_{m,sol}$) is known.[18] E_ms calculated in this way are in good agreement with the observed data, representing 73% of the E_m range found in the proteins. However, adding an additional 160 mV to all His-Met *c* hemes significantly improves the results, yielding a slope of 0.97 and R^2 of 0.93 for the comparison of calculated and experimental data. Possible sources of the error are discussed. Hemes can be classified by their heme type (*a*, *b*, and *c* here) and axial ligands (bis-His, His-Met, and aquo-His here).[59] Hemes in different categories are found in different E_m regions and the interactions that contribute to the E_m shifts are described for each class. The sensitivity of the calculations to the parameters used was tested by comparing the results with different heme partial charges and with a protein dielectric constant of 4 and 8. The calculated E_ms are found to be not very sensitive to these changes.

METHODS

Protein selection

All structures were obtained from the Protein Data Bank.[60] Forty-two different heme-containing proteins (63 pdb files, 96 structures, 141 hemes) with experimental E_ms spanning 800 mV were examined (See Fig. 1, Figure S1). These proteins range in size from the 76 residue cyt. c_{553} to the 1212 residue bc_1 complex. Most structures were solved by X-ray crystallographer with a resolution of 2.5 Å or better. When there are multiple copies of a protein in one PDB file, each independent copy was analyzed separately, keeping all the results. Three NMR

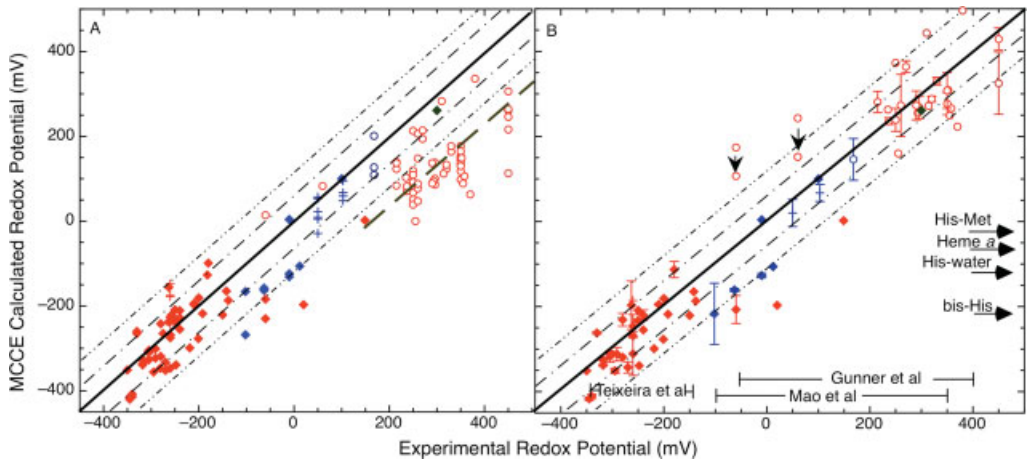

Figure 1

MCCE calculated vs. experimental redox potential (mV).[111–134] (**a**) All $E_{m,calc}$ vs. $E_{m,expt}$ (mV). (**b**) Averaging $E_{m,calc}$ for all proteins with multiple structures available (mV). Error bars show standard deviation of calculated E_ms. A +160 mV offset is added to all calculated His-Met *c* hemes. The two black arrows pointing downwards indicate the shifts in $E_{m,cal}$s when the propionic acids were forced to be fully ionized in *Rps. viridis* reaction centers and *B. pasteurii* cyt c_{553} (See Results and Discussion). ◆(green): bis-His *a* type. ◆(blue): bis-His *b* type. ◆(red): bis-His *c* type. ○(blue): His-Met *b* type. ○(red): His-Met *c* type. +(blue): aqua-His *b*. +(red): aqua-His *c*. Central black solid line is where experimental and calculated E_ms are equal. The dashed line in (a) is the 160 mV offset for His-Met *c*-type. The black dot dashed and double dot dashed lines are the ±60 and ±120 mV error lines. The arrows pointing to the *y*-axis show the $E_{m,sol}$s used in this calculation, which are −220 mV for bis-His, −120 mV for His-water, −60 mV for bis-His *a* and −15 mV for His-Met. The range of previous heme E_ms calculations is also shown.[18,20,22]

structures were considered here (cytochrome b_5 1AW3, cytochrome b_5 1B5A, and cytochrome b_{562} 1QPU), all of which contain a single structure in the PDB file. With the exception of a single heme *a* in cytochrome *c* oxidase, there are only *b*- and *c*-type hemes included, with ligand type bis-His, His-Met, or aquo-His. All crystal waters were deleted from the structures. Five coordinate hemes, with a single protein ligand, were fitted with an aquo ligand. This can be a water or hydroxyl, with a pK_a that is dependent on the heme oxidation state.[61] A dielectric constant of 80 was applied to the surrounding water. Protein cavities were filled with continuum water. The default value for the protein dielectric constant was four.

Three membrane proteins are included: bovine bc_1 complex, *Rhodobacter sphaeroides* cyt. *c* oxidase, and the *Rhodopseudomonas viridis* reaction center. The hemes in the reaction center are in an extra-membrane cytochrome *c* subunit, which was isolated and analyzed independently. These heme E_ms are not affected by removing the other three transmembrane subunits (Gunner unpublished results). A membrane slab of ∼35 Å was built for cyt. *c* oxidase and the bc_1 complex using the program IPECE.[54,62] IPECE is embedded in MCCE as an optional procedure. Membranes were assigned a dielectric constant of four. In cyt *c* oxidase, the E_m for the bis-his heme *a* was calculated with all other cofactors fixed in their oxidized states.

MCCE

MCCE is a semi-empirical method combining classical continuum electrostatics and molecular mechanics.[36,38,63] It samples the ionization state of each residue and cofactor in the protein as a function of E_h and pH. Version MCCE2.4 was used here. In MCCE, the protein backbone and the heme ring heavy atoms are fixed. MCCE generates rotamers in 60° steps around each rotatable bond for both ionizable and nonionizable sidechains and the heme propionic acids. Each possible conformation or ionization state for a residue is called a conformer. All pairs of conformers with only modest clashes (<5 kcal/mol) have their positions optimized. All acidic and basic residues have conformers for the neutral and ionized states and multiple hydroxyl positions are found in different conformer. Solution of the finite-difference Poisson-Boltzmann equation using DelPhi[45] yields an energy look-up table, which contains the electrostatic conformer–conformer pairwise interactions and reaction field energy for each conformer. A salt concentration of 0.15*M*, a water probe radius of 1.4 Å and a 2.0 Å Stern ion-exclusion radius were used. Protein residues were assigned PARSE charges and radii.[64] Focusing runs give a final resolution better than 2.0 grids/Å.[65] The nonelectrostatic van der Waals interactions and torsion energies were calculated with standard AMBER parameters.[66] For a protein with ∼110 residues, ∼1200 conformers are made, with each conformer representing a choice of atomic position and ionization state for a sidechain, chain termini, or cofactor. For every protein microstate, a single conformer was selected for each residue. Monte Carlo sampling calculates the Boltzmann distribution of all conformer ionization states and positions

at 25°C. Each calculated result reported here is the average of two independent Monte Carlo sampling runs. The total energy for one microstate (ΔG^n) is:

$$\Delta G^{\mathrm{n}} = \sum_{i=1}^{M} \delta_{n,i}\{[2.3 m_i RT(pH - pK_{\mathrm{sol},i}) + n_i F(E_{\mathrm{h}} - E_{\mathrm{msol,i}})] + (\Delta\Delta G_{\mathrm{rxn},i} + \Delta G_{\mathrm{pol},i})\} + \sum_{i=1}^{M} \delta_{n,i} \sum_{j=i+1}^{M} \delta_{n,i}(\Delta G_{ij}) \quad (1)$$

RT is 0.59 kcal/mol, and F is the Faraday constant. $\delta_{n,i}$ is one for the conformer i that is occupied and 0 for all other conformers in the residue. m_i is 1 for bases, −1 for acids, and 0 for all other groups. n_i is the number of electrons. M is the total number of conformers in the protein. $pK_{\mathrm{sol},i}$ and $E_{\mathrm{msol},i}$ are the pK_a and midpoint potential in the solution for residue. $\Delta\Delta G_{\mathrm{rxn},i}$ is the desolvation energy, the loss of reaction field energy when conformer i is moved from solution to protein. $\Delta G_{\mathrm{pol},i}$ is the pairwise electrostatic and nonelectrostatic interaction between the conformer i and the backbone dipoles. ΔG_{ij} is the electrostatic and nonelectrostatic interaction between two conformers. A detailed description of the method can be found in.[22,36,38,54,55]

Midpoint reduction potential (E_m) calculation

MCCE follows the percentage of group ionization for each residue or cofactor as a function of pH or E_h [Eq. (1)]. The midpoint redox potential is the E_h, where half of the hemes are oxidized. The MCCE procedure keeps all protonation states in equilibrium with the heme as it changes redox state during the titration. This allows the proton uptake coupled to electron transfer to be determined from the number of protons bound to the ionizable groups as a function of the cofactor redox state. The default calculations are carried out at pH 7. The following proteins were analyzed at alternate pH where the E_m was measured: cyt c_3 3CAO, 3CAR at pH 7.6; cyt c_3 1CZJ at pH 8.1; cyt c 1M1R at pH 9.0.

The influence of the protein on the E_m can be determined from:

$$E_m = E_{m,sol} - \Delta G_{protein}/nF \quad (2)$$

$\Delta G_{protein}/nF$ is the effect of the protein on the free energy of the redox reaction.[31,56,22] This term can be decomposed in MCCE calculation as:

$$\Delta G_{protein} = (\Delta\Delta G_{rxn} + \Delta G_{pol}) + \Delta G_{res,prop} + \Delta G_{res,prot} \quad (3)$$

This incorporates the difference in the loss in reaction field energy (desolvation energy) moving from solvent to protein ($\Delta\Delta G_{rxn}$), the change in interaction with the backbone dipoles (ΔG_{pol}) and contributions from the electrostatic interaction with the propionates ($\Delta G_{res,prop}$) and the rest of the protein ($\Delta G_{res,prot}$). In each case, the difference between the interaction of the oxidized and reduced heme with the protein determines the resultant E_m shift. $\Delta\Delta G_{rxn}$ always destabilizes heme oxidation, raising E_ms[42,43,67] because the solvation energy loss is always greater for the more highly charged oxidized heme. Ionized propionates always have favorable interaction ($\Delta G_{res,prop}$) with the heme, lowering the E_ms. ΔG_{pol} and $\Delta G_{res,prot}$ depend on the protein context. They are as likely to favor the reduced as the oxidized heme.

Heme-ligand complex

Heme, its axial ligand sidechains and, for the *c*-type hemes, the Cys sidechains that are covalently bound to the hemes, are treated together as a single unit with an oxidized or reduced conformer. The backbone atoms for the residues that function as ligands remain as part of the protein backbone. The two propionates are treated as independently ionizable groups.

The measured E_m of −220 mV (vs. SHE) of bis-His microperoxidases (MPs) in solution was used as the solution E_m ($E_{m,sol}$) for the bis-His hemes.[68] The $E_{m,sol}$ of −15 mV derived from site-directed mutation from bis-His to His-Met axial ligands[69,70] was used for His-Met hemes (see Mao J, Hauser K, Gunner MR[22] for a more complete discussion).

Five-coordinate hemes bind a water or hydroxide as a sixth ligand. Solution pK_a ($pK_{a,sol}$) and $E_{m,sol}$ of this heme complex were also taken from the measurements on microperoxidase.[71,72] The hydroxyl $pK_{a,sol}$ is 9.6 in the ferric and 10.9 in the ferrous heme. $E_{m,sol}$ is −120 mV for His-water heme and −200 mV for hydroxyl-His heme.[61,73,74]

The reference reaction field energy ($\Delta G_{rxn,sol}$) of the heme complex was precalculated by DelPhi for each ligand-heme complex by moving the heme with the axial ligands from dielectric constant of 4 to 80 in the reduced and the oxidized states (see Table II). In calculations with a protein dielectric constant of 8, the heme complex was moved from $\varepsilon = 8$ to 80 in Delphi to generate $\Delta G_{rxn,sol}$. The Cys peripheral ligands were included in the atomic structure of the *c*-type heme complex. The propionic acids, which are considered as independently ionizable groups, were removed. The same procedure was carried out to generate the solution reaction field energy for the ionized and neutral acids and bases.[38]

The propionates are given at least two protonated conformers, with a proton on either carboxylic oxygen, and one deprotonated conformer.[22] Each of these can have multiple heavy atom rotamers if these can be accommodated in the protein structure. Protonated conformers have a total charge of zero, whereas deprotonated ones have

−1.00. A standard solution pK_a of 4.9 for carboxyl group was used for propionates.[75] The reference reaction field energies are −2.5 kcal/mol for the protonated conformers and −18.23 kcal/mol for the deprotonated conformer.

The default calculations use a metal centered charge distribution on the hemes.[18] This has −0.5 charge on each heme ring nitrogen atom and +2 or +3 charge on the iron in the reduced or oxidized state, respectively.[18] Ligand side chains have PARSE charges on each atom, with a net charge of zero in both the neutral and ionized heme complex. In addition, a Mulliken charge set was obtained by Gaussian03 calculation with HF/6-31G and B3LYP/6-31G basis sets for the His-Met *c*-type heme[76] and results were compared with those obtained with the metal centered charge (see Table SI, SII). Here charges of +1.20 and +1.34 were assigned to the iron in reduced and oxidized heme. All ligands, His, Met, and Cys, have a nonzero net charge in each state. The total heme complex (including two propionates) has −2 and −1 charge. With the heme reduced, the covalently attached propionic acid each has an assigned net charge of −1. However, when the heme is oxidized there is a charge shift diminishing the assigned propionic acid charge to −0.81. A −1.00 charge is assigned to each of the propionates in the calculation regardless of the heme oxidation state. The missing +0.38 charge was evenly added to each atom in the plane of the oxidized heme. Electrostatic potential charge (ESP) and natural bond orbital (NBO) charges for the bis-His *c*-type heme were also obtained using Jaguar[77] (Zhang J, Gunner MR, in preparation). The iron should have a positive atomic charge. Thus with positively charged heme iron of +0.69 and +1.04 in reduced and oxidized, NBO charges appear to be physically reasonable. In contrast, ESP charges put –0.65 and –0.23 charge on iron in reduced and oxidized.

RESULTS AND DISCUSSION

Midpoint redox potentials ($E_{m,calc}$) were obtained using MCCE on 141 hemes in 42 different proteins. Where available, several atomic structures were used for the same protein: 93 individual structures from 63 pdb files were analyzed. The $E_{m,calc}$ for each heme is found in the supplementary material (see Table SIII). Calculated and experimental results were compared (Fig. 1, Fig. S1). The measured E_ms ($E_{m,expt}$) range from −350 mV to 450 mV. The proteins studied include the soluble proteins: cytochromes *c*, c_2, c_3, c_4, c_{549}, c_{550}, c_{551}, c_{552}, c_{553}, c_6, c_7, c'' cytochromes b_5, b_{562}; hemoglobin, myoglobin; cytochrome *c* peroxidase; quinohemoprotein amine dehydrogense (the diheme cytochrome *c* domain)[78]; and the membrane proteins: reaction center, bc_1 complex and cytochrome *c* oxidase. Twenty-seven of the forty-two proteins have one heme only. Others include six di-heme proteins; two tri-heme proteins, and seven tetra-heme proteins.

Contribution of the different electrostatic energy terms to $E_{m,calc}$

MCCE interprets the *in situ* midpoint redox potential as shifted from solution by the protein because of the loss in the self (reaction field) energy ($\Delta\Delta G_{rxn}$), which always favors heme reduction raising E_ms,[42,43] and pairwise electrostatic interactions with backbone dipoles, propionic acids, and charged or polar side chains (ΔG_{pol}, $\Delta G_{res,prop}$, and $\Delta G_{res,prot}$) [Eq. (3), Table I, Fig. 2].[22,61,62] The method allows decomposition of these electrostatic terms to determine what features yield the observed electrochemistry in each protein. This new analysis of proteins with an E_m range of 800 mV overturns some conclusions from an earlier MCCE study analyzing a group of higher potential hemes with $E_{m,expt}$ spanning 450 mV from −102 to 350 mV.[22]

$\Delta\Delta G_{rxn}$: Moving into the protein from the water always destabilizes the more highly charged oxidized heme more than the reduced, raising the E_m.[42,43] Deeply buried hemes suffer a bigger loss than more exposed ones. The variation of heme exposure to solvent has been suggested to be a primary determinant of the in site E_m.[79–81] However, previous CE[82] and MCCE[22] studies found a small range of $\Delta\Delta G_{rxn}$ of only ~130 meV in hemes with an $E_{m,expt}$ range of ~450 mV and thus suggested that variation in solvation energy is not the dominant factor in determining heme E_ms. Over the wider E_m range covered here, $\Delta\Delta G_{rxn}$ varies from 3 meV in small soluble tetra-heme cytochrome *c* protein ($E_{m,expt}$ −248 mV)[83] to 305 mV in the sperm whale myoglobin ($E_{m,expt}$ 50 mV).[84] This 302 meV range, while significant, is still insufficient to account for the whole range of $E_{m,expt}$ of 800 mV. In addition, the correlation between $\Delta\Delta G_{rxn}$ and $E_{m,expt}$ shows a slope of only ~0.2 with an R^2 of 0.493 [Table I, Fig. 2(a)].

ΔG_{pol}: Each amino acid has an associated backbone amide group, which has a dipole moment larger than that of water. Earlier electrostatic surveys of protein electrostatics found that on average the protein backbone dipoles are oriented in all proteins to make the interior more positive.[85] In previous MCCE analysis of heme E_ms, interactions with the protein backbone were always found to destabilize heme oxidation, raising the redox potential.[22] Here, as the potential range is expanded to low potential hemes and new high potential proteins are added, there are hemes found where the backbone dipoles favor oxidation. ΔG_{pol} ranges from −158 meV in *Thermosynechococcus elongatus* cytochrome c_{550} ($E_{m,expt}$ −240 mV[86]) to 187 meV in *Rhodobacter sphaeroides* cytochrome c_2 ($E_{m,expt}$ 355 mV[87]). However, overall there is little correlations between ΔG_{pol} and $E_{m,expt}$ [Table I, Fig. 2(b)].

Table I
Experimental and MCCE Calculated E_m Range for Each Ligand and Heme Type (mV)

	No. proteins	No. pdb		$E_{m,expt}$	$E_{m,cal}$	$\Delta\Delta G_{rxn}$	ΔG_{pol}	$\Delta G_{res,prop}$	$\Delta G_{res,prot}$
All	42	63	Range	[−350,450]	[−420,336]	[3,305]	[−158,187]	[−522,30]	[−261,507]
			AVE ± STD	0 ± 263	−77 ± 207	113 ± 78	24 ± 74	−128 ± 90	53 ± 107
			Slope	n/a	0.728	0.198	0.173	−0.165	0.199
			R^2	n/a	0.898	0.493	0.373	0.223	0.302
			Slope[a]	n/a	0.969	n/a	n/a	n/a	n/a
			R^{2a}	n/a	0.931	n/a	n/a	n/a	n/a
bis-His *a*	1	1	Range	300[b]	261	205	131	−522	507
bis-His *b*	3	7	Range	[−102,100]	[−268,100]	[85,280]	[−23,139]	[−243,−47]	[−77,345]
			AVE ± STD	−12 ± 69	−85 ± 116	147 ± 91	71 ± 59	−120 ± 70	54 ± 160
			Slope	n/a	0.913	0.361	0.267	−0.490	0.988
			R^2	n/a	0.358	0.107	0.114	0.322	0.251
bis-His *c*	14	16	Range	[−350,149]	[−420,2]	[3,110]	[−158,114]	[−185,30]	[−146,216]
			AVE ± STD	−230 ± 104	−260 ± 85	47 ± 30	−13 ± 62	−89 ± 40	17 ± 73
			Slope	n/a	0.674	0.046	0.272	−0.058	0.427
			R^2	n/a	0.568	0.024	0.164	0.020	0.371
His-Met *b*	1	2	Range	168	146	117	18	−44	70
His-Met *c*	24	33	Range	[−60,450]	[0,336]	[86,283]	[−84,187]	[−332,3]	[−69,348]
			AVE ± STD	287 ± 101	133 ± 77	169 ± 29	56 ± 75	−168 ± 96	92 ± 77
			Slope	n/a	0.490	0.089	0.239	−0.008	0.173
			R^2	n/a	0.336	0.091	0.083	0.000	0.046
aqua-His *b*	2	10	Range	50,103	20,67	246,204	50,40	−139,−117	24,80
aqua-His *c*	1	1	Range	−260	−186	199	40	−147	−198
b	6	19	Range	[−102,168]	[−268,201]	[77,305]	[−23,139]	[−243,−37]	[−77,345]
			AVE ± STD	28 ± 86	−31 ± 127	161 ± 81	59 ± 50	−113 ± 61	55 ± 128
			Slope	n/a	1.344	0.183	−0.143	0.003	0.593
			R^2	n/a	0.687	0.030	0.064	0.000	0.234
c	34	44	Range	[−350,450]	[−420,336]	[3,283]	[−158,187]	[−332,30]	[−261,348]
			AVE ± STD	−10 ± 277	−91 ± 211	101 ± 68	17 ± 75	−124 ± 79	46 ± 88
			Slope	n/a	0.714	0.190	0.175	−0.156	0.180
			R^2	n/a	0.923	0.653	0.399	0.239	0.347
bis-His	18	24	Range	[−350,300]	[−420,261]	[3,280]	[−158,139]	[−522,30]	[−146,507]
			AVE ± STD	−183 ± 155	−219 ± 141	69 ± 74	3 ± 70	−104 ± 81	35 ± 116
			Slope	n/a	0.755	0.289	0.301	−0.252	0.406
			R^2	n/a	0.749	0.452	0.372	0.283	0.348
His-Met	24	33	Range	[−60,450]	[0,336]	[77,283]	[−84,187]	[−332,3]	[−69,348]
			AVE ± STD	282 ± 102	133 ± 76	167 ± 30	54 ± 74	−164 ± 97	91 ± 75
			Slope	n/a	0.425	0.121	0.264	−0.127	0.172
			R^2	n/a	0.279	0.131	0.109	0.010	0.050
aqua-His	3	11	Range	−260,50,103	−186,20,67	199,246,204	40,50,40	−147,−139,−117	−198,24,80
Low-potential	13	16	Range	[−350,−102]	[−420,−99]	[−10,223]	[−158,114]	[−206,30]	[−261,101]
			AVE ± STD	−251 ± 63	−267 ± 73	50 ± 37	−12 ± 64	−86 ± 38	−3 ± 64
			Slope	n/a	0.877	0.015	0.561	0.176	0.140
			R^2	n/a	0.463	0.000	0.272	0.055	0.012
Mid-potential	10	22	Range	[−63,168]	[−230,201]	[9,305]	[−23,139]	[−243,−31]	[−74,345]
			AVE ± STD	35 ± 78	−28 ± 118	146 ± 78	41 ± 51	−120 ± 59	75 ± 121
			Slope	n/a	1.213	0.258	−0.127	0.108	0.490
			R^2	n/a	0.508	0.045	0.039	0.022	0.127
High-potential	23	31	Range	[215,450]	[0,336]	[86,283]	[−84,187]	[−522,3]	[−69,507]
			AVE ± STD	314 ± 56	148 ± 85	178 ± 50	63 ± 76	−188 ± 116	116 ± 109
			Slope	n/a	0.737	0.210	0.246	0.092	0.228
			R^2	n/a	0.362	0.118	0.048	0.002	0.026

The value for heme *a* from *Rb. sphaeroides* is used in the figures and data analysis.[101]
MCCE calculated energy terms as discussed in methods (meV) (see Eqn 3).
[a]Slope and R^2 for value vs. $E_{m,expt}$ after adding *a* +160 mV offset for His-Met *c* type hemes.
[b]$E_{m,expt}$ for bis-His *a* varies from 300 mV[101], 340 mV[135] to 430 mV[136] in different species.

Small differences in protein structure can lead to significant differences in calculated ΔG_{pol}. For example, *B. taurus* cytochrome b_5 ($E_{m,expt}$ −10 mV[88]) and *T. elongatus* cyt c_{550} ($E_{m,expt}$ −240 mV[86]) both have a Pro adjacent to the His axial ligand, which makes the most significant contribution to ΔG_{pol} (see Fig. 3). In cytochrome b_5, the Pro raises the E_m by ≈50 mV, whereas in cytochrome c_{550} the analogous residue lowers it by a similar amount. This difference results from the orientation of the Pro carbonyl, which points towards the heme in cyt. c_{550} and away in b_5. The backbone is the one structural element that is not optimized in MCCE conformational

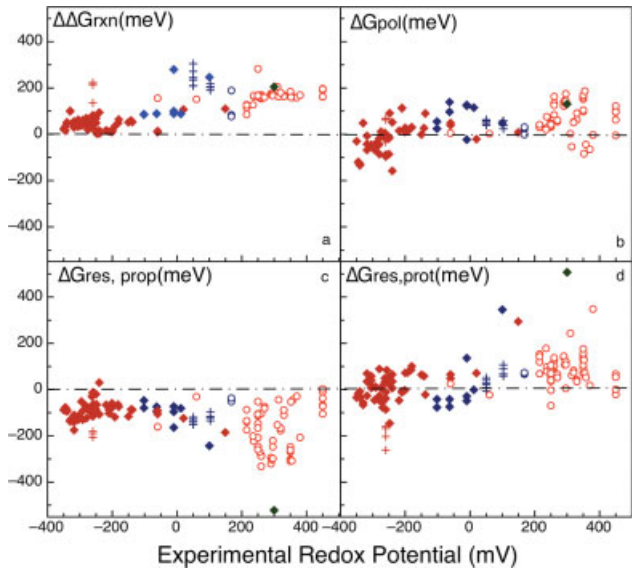

Figure 2

Energy terms contributing to the $E_{m,calc}$ vs. $E_{m,expt}$. (**a**) $\Delta\Delta G_{rxn}$: loss of reaction field energy (desolvation energy); pairwise interaction with (**b**) ΔG_{pol}: backbone dipoles; (**c**) $\Delta G_{res,prop}$: propionic acids; (**d**) $\Delta G_{res,prot}$: sidechains. Symbols are the same as in Figure 1. The slope and R^2 values for each figure can be found in Table I.

sampling. The comparison of the results calculated with different atomic structures provides the only way to access the variability of ΔG_{pol} for a given protein (Table SIII).

$\Delta G_{res,prop}$: All hemes have two propionic acids as peripheral ligands. When ionized, they lower the midpoint potential, favoring heme oxidation. Strong unfavorable interactions between the two propionates can keep them from both being fully ionized. The more deeply buried acids lose reaction field energy, which destabilizes ionization and also increase the strength of the repulsion between the two propionates.

Oxidation of the hemes always shifts the pK_a of the acid down, leading to proton release if the pK_a is near the solution pH.[22,89,28] The net charge on the two propionic acids is <-1 (>50% ionized) in 114 out of 141 (81%) hemes in the reduced state, with 40% of the propionic acids more than 90% ionized. When the hemes are oxidized now 129 hemes (91%) have their propionic charge between -1 and -2 and 65% are >90% ionized. The associated proton release on heme oxidation makes the propionic acids important contributors to the pH dependence of many heme E_ms.

The $\Delta G_{res,prop}$ ranges from ≈ 0 to -522 meV. This is calculated at pH 7 at the E_h where the heme is 50% ionized in Monte Carlo sampling (i.e. $E_h = E_{m,calc}$) [Eq. (1)]. The lowest value is -522 meV for a deeply buried propionic acid on Heme *a* in cytochrome *c* oxidase. The deeply buried acid remains charged due to its interactions with two Arg (R481, R481) less than 3 Å away. Another nearby Arg (R52), a Mg^{+2}, and a Ca^{+2} ions also help to stabilize both the ionized heme acids. Of course the positive potential from the nearby cations will raise the potential at the heme. With the exception of cytchrome *c* oxidase, the most favorable heme-propionate acid interaction is -332 mV in cyt *c* ($E_{m,expt}$ 260[90]). In the low potential cyt c_{550} ($E_{m,expt}$ -240 mV[86]) and high potential cyt c_4 ($E_{m,expt}$ 450 mV[91]), the propionates are fully protonated at pH 7, so the polar, neutral acids have very small unfavorable interaction with the oxidized heme of 30 and 3 meV, respectively.

The heme redox potential correlates poorly with the fractional propionate ionization or with the electrostatic interaction between these attached acids and the rest of the heme [Table I, Fig. 2(c)]. Interestingly, there is a weak negative correlation between $\Delta G_{res,prop}$ and $E_{m,expt}$. This arises because deeply buried, ionized propionic acids, which themselves lower the E_m, must in turn

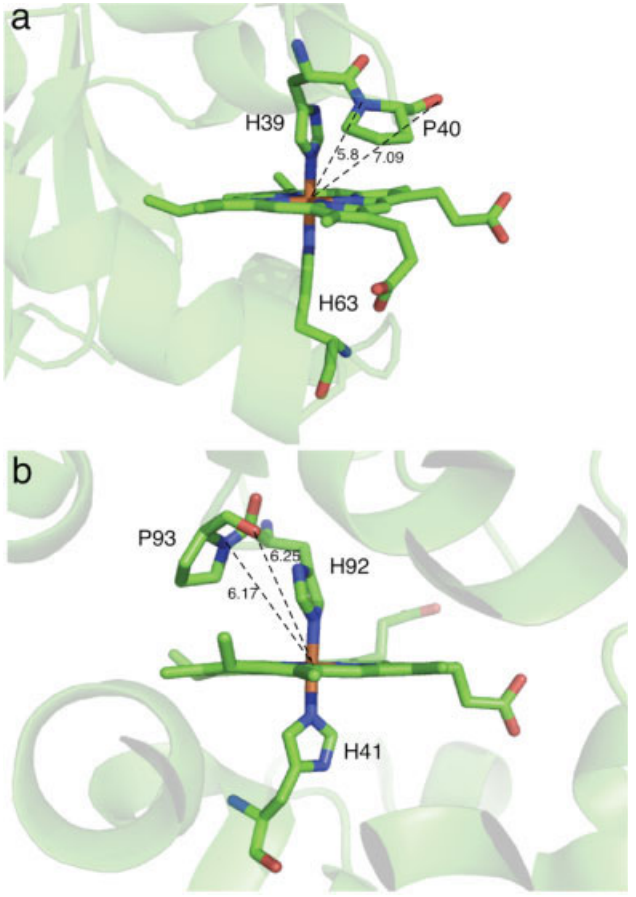

Figure 3

Residue backbone dipoles with strong interaction with the heme. (**a**) bovine b_5 1CYO with a total ΔG_{pol} of 123 meV. (**b**) Cyt. c_{550} 1MZ4 with a total ΔG_{pol} of -158 meV. Distances between the iron and the carbonyl group, amine are labeled in Å. The two axial Histidine ligands and one Proline adjacent to the ligand are shown.

be surrounded by cations which will tend to raise the heme E_m.

Earlier studies by Mao calculated that, in reduced cytochromes, the acids have an interaction with the hemes ranging from −40 to −170 meV, whereas with an oxidized heme, it is more favorable, ranging from −60 to −270 meV.[22] The interactions reported here on the same proteins are more favorable. The differences are due to improvements in the MCCE methodology. The earlier calculations used an ad hoc SOFT function,[38] which weakened strong electrostatic interactions. This was necessary because of the added low dielectric material introduced by the multiconformation method which has all conformers present when calculating the pairwise interactions.[36,38] In contrast, the current method uses a more accurate, physical correction for errors in the boundary conditions. The pairwise electrostatics interactions between the single conformers from the original structure are considered correct. The same interaction is also calculated in the multiconformation structure and correction is defined to recover the correct value. The same factor applied to all the conformer–conformer electrostatics pairwise interactions between the two residues (see details in Song Y, Mao J, Gunner MR, in preparation).

$\Delta G_{res,prot}$: The ionizable and polar amino acids in the protein also modify the heme redox potential via electrostatic pairwise interactions. Here, $\Delta G_{res,prot}$ varies from −261 meV in the di-heme peroxidase ($E_{m,expt}$ −260 mV[16]) to 507 meV in cyt. *c* oxidase, much larger than the range from −60 to 165 meV found by Mao J and coworkers.[22] As seen in Table I and Figure 2(d), there is no correlation between the $\Delta G_{res,prot}$ and redox potential.

Comparison of the electrochemistry of the different classes of heme proteins

b- *vs. c*-type

Hemes are attached to the protein by purely nonbonded interactions in the *a*- or *b*-type hemes or via two Cys linkages in the *c*-type hemes. In addition, the protein provides one or two axial ligands to the heme. The *b*-type heme, the most common heme tetrapyrrole macrocycle, is the structure from which heme *a* and *c* are derived.[17,59] The dataset here includes one *a*-type heme, 118 *c*-type hemes, and 22 *b*-type hemes. Only bis-His, His-Met, and aquo-His hemes with measured E_ms were examined here producing a dataset with more *c*-type than *b*-type hemes. The *b*-type hemes are more likely to be found with other ligands.[59]

The *b*- and *c*- type hemes are found clustered in different E_m ranges. The *b*-type hemes have their E_ms in the middle of the E_m range measured for heme proteins, whereas *c*-type hemes are mainly found either above 250 mV or below −100 mV. Thus, the *c*-type hemes span an 800 mV $E_{m,expt}$ range, from −350 mV in *Desulfovibrio desulfuricans* Norway cytochrome c_3[92] to 450 mV in *Nitrosomonas europaea* peroxidase,[16] whereas *b*-type hemes span less than 300 mV, ranging from −102 mV in *Rat microsonal* cytochrome b_5[93] to 168 mV in *Escherichia coli* cytochrome b_{562}.[94] It can be seen that each of the electrostatic terms are larger for the bis-His *b* type hemes than for the more exposed bis-His *c*-type hemes (Table I). The covalent attachment of the heme to the protein via two Cys linkages has been assumed to modify the E_m only by the small shifts in the reference reaction field energy. This is supported by the small shift in E_m measured when the *c*-type heme in cytochrome c_{552} is mutated to a *b*-type heme by replacing both Cys ligands by Ala.[95] Thus, the difference between the $E_{m,calc}$ for the bis-His *b*- and *c*-type hemes is calculated to be solely due to the MCCE electrostatic terms.

Independent of the axial ligation, the E_ms for the *b*-type hemes are ≈200 mV more positive than the $E_{m,sol}$ for the respective ligand type (Fig. 1, Table I). The heme ligand types studied here have $E_{m,sol}$ of −220 mV, −120 mV, and −15 mV and for bis-His, aquo-His, and His-Met ligands, respectively. The average $E_{m,expt}$ is −12 ± 69 mV for bis-His hemes (a shift of 208 mV from $E_{m,sol}$), 168 mV for the single His-Met heme (183 mV shift), and 76 ± 27 mV for aquo-His hemes (196 mV shift). A positive E_m shift, with its destabilization of the oxidized state of the heme relative to solution, indicates the protein binds the reduced heme more tightly than the oxidized form. A 200 mV E_m shift represents a 2000 fold difference in affinity, representing a 4.5 kcal/mol difference in binding energy.[55,96] In contrast, for *c*-type hemes, the bis-His ligated hemes have an average $E_{m,expt}$ of −230 ± 104 mV, shifting on average only 10 mV from $E_{m,sol}$. Thus, on average, the oxidized and reduced states are bound with similar affinity. The single aquo-His *c*-heme has an $E_{m,expt}$ of −260 mV lower than the $E_{m,sol}$ of −120 mV, Whereas the His-Met hemes have an average E_m more than 500 mV higher. Their average $E_{m,expt}$ of 287 ± 101 mV represents a shift of 302 mV from $E_{m,sol}$.

The reason for the biological selection of *b*- and *c*-type hemes for different functions is still a matter of debate.[17,96–98] With two covalent thioether attachments, the *c*-type hemes will bind essentially irreversibly to the protein. The covalent attachment appears to allow an increase in the ratio of heme to protein. This seems especially important for the group of low potential multiheme proteins. For example in the c_3 proteins, four *c*-type hemes are successfully accommodated into a compact but elegant soluble protein of only ∼110 residues. Overall the low potential *c* cytochromes have from 23 to 135 amino acids/heme. It is hard to imagine that without the covalent attachment there would be sufficient nonbonded interactions between each heme and the protein. However, the small covering of protein does not interact much with the heme, yielding the smallest values for each of the MCCE electrostatic energy terms (Table I,

Fig. 2). Thus, the low potential *c*-type cytochromes have relatively small shifts in E_m from $E_{m,sol}$.

The high potential *c*-type hemes, which use His-Met ligation, may use a covalently bound heme for a different reason. The His-Met ligands have a more positive $E_{m,sol}$. However, on average the *in situ* $E_{m,expt}$s are 300 mV more positive than the His-Met $E_{m,sol}$ of −15 mV. This indicates the oxidized heme binds 10^6 times more weakly than the reduced cofactor. In general, the oxidized hemes tend to be more weakly bound, potentially destabilizing the protein.[99] As suggested by Gibney and coworkers,[96] the covalent attachment in the high potential c-type proteins may be needed to ensure reversible redox reactions with a very positive E_m shift without heme loss. These proteins with their greatly shifted E_ms tend to have large values for all MCCE electrostatic energy terms.

The *c*-type hemes do generally show somewhat better R^2 values than *b*-type hemes for the comparison of the decomposed electrostatic energy terms with the experimental E_ms (Table I, Fig. 2). However, this is largely due to the fact that *c*-type hemes cover a significantly larger range of E_ms. Analyzing an E_m range from −138 to 149 mV in *c*-type hemes similar to that found in the *b*-type, the slopes for each energy term in the *c*-type hemes do not change much. However, the R^2 values drop significantly. They are now 0.225 and 0.4 for $\Delta\Delta G_{rxn}$ and ΔG_{pol}, a little better for *b*-type hemes, and 0 and 0.027 for $\Delta G_{res,prop}$ and $\Delta G_{res,prot}$, which are even worse.

bis-His vs His-Met *vs aquo-His*

The sixty-four His-Met type hemes have an $E_{m,expt}$ span of 510 mV, from −60 mV (in tetra-heme *Rhodopseudomonas viridis* reaction center[100]) to 450 mV (in di-heme *Nitrosomonas europaea* peroxidase[16]). In the sixty-three bis-His type hemes, $E_{m,expt}$ varies from −350 mV (in tetra-heme *Desulfovibrio desulfuricans* Norway[92]) to 300 mV (in *Rhodobacter sphaeroides* cytochrome *c* oxidase[101]). The fourteen aquo-His ligated hemes have a smaller $E_{m,expt}$ range from −260 mV (*Nitrosomonas europaea* peroxidase[16]) to 103 mV (*monoeric clam* hemoglobin[84]). There are only two proteins with aquo-His *b* hemes, and one protein each with aquo-His *c* or His-Met *b* hemes. Overall, although hemes in proteins have a total E_m range of 800 mV here, proteins with a particular heme and ligand type are likely to be found in a range of 200–500 mV. In the calculations, the different axial ligand types are assumed to add an nonelectrostatic offset via the differences in $E_{m,sol}$.

For the *c*-type hemes, the low and high potential hemes can be compared. Their average E_ms vary by ∼500 mV. This 500 mV range of $E_{m,expt}$, equivalent to an 11.3 kcal/Mol shift in the reaction equilibrium constant is well calculated by the MCCE method (see Fig. 1).The high potential hemes use His-Met rather than bis-His ligands, raising $E_{m,sol}$ by 205 mV; the high potential hemes have ≈120 mV less solvation energy, 150 mV more positive interaction with the backbone dipoles and the sidechains. The more buried *c*-type hemes also have larger interactions with their propionic acids lowering the potential by ≈80 mV. However, as will be described below MCCE does not account for all of the destabilization of the oxidized His-Met hemes, resulting in $E_{m,calc}$ which are systematically lower than $E_{m,expt}$ [Fig. 1(a)].

There are several hemes, which are shifted more significantly by the protein than the norm for the given heme and ligand type and these pose the best test of the MCCE calculation method. Although the majority of bis-His *c* type hemes are at low potential, ranging from −350 to −60 mV, one in the 400 residue reaction center cytochrome *c*-subunit and one in the 500 residue heme binding subunit of the quinohemoprotein amine dehydrogenase (QH-AmDH) have a much higher $E_{m,expt}$ of 20 and 149 mV, respectively. These are calculated to have E_ms near 0 mV, well separated from the low potential bis-His *b*-type hemes. Traditionally, hemes are predicted to move to high potential because of the loss of reaction field energy, which destabilizes the oxidized heme.[42,43,102] This is in agreement with our observation here. The electrostatic analysis of these two high potential bis-His *c*-type hemes shows that they are better buried in the protein than the average bis-His *c*-type heme with $\Delta\Delta G_{rxn}$ of ≈60 meV, ≈80 meV more positive than the average value for this group (Table I). However, this is not enough to raise the heme E_m in QH-AmDH by ∼400 mV from the averaged E_m of its type. Therefore, other forces must be enhancing the heme reduction. The pairwise electrostatic interactions with the protein sidechains are also much stronger in QH-AmDH. Four Arginines (R42, R102, R108, R114) near the heme make a total contribution of ∼400 meV raising the $E_{m,calc}$. However, this is largely canceled by a ∼130 meV interaction with the nearby heme propionic acids.

His-Met *c*-type hemes usually have high $E_{m,expt}$, in the range of 250 to 450 mV. There are two with unusual low redox potentials, at 60 meV in cyt. c_{553} and −60 mV in the *Rb. viridis* reaction center. Solvent heme exposure has been suggested to be one of the most important factors responsible for the uncommon low cyt. c_{553} E_m.[81] However, the calculations here show that $\Delta\Delta G_{rxn}$ of 152 meV is only ∼20 meV lower than the average of His-Met *c* type. Comparing these hemes with the average for the members of their class (Table I) shows that ΔG_{pol} and $\Delta G_{res,prot}$ are the terms which yield the lowered $E_{m,calc}$.

Error analyses and parameter sensitivity

MCCE calculation results are in reasonable agreement with the experimental data. The slope comparing all experimental and calculated values is 0.73 with an intercept at −77 mV and a reasonable R^2 of 0.90. Thus, the calculations are able to reproduce an E_m range of 756 mV,

from −420 mV in cytochrome c_3 to 336 mV in reaction center. By using the experimental values for $E_{m,sol}$ for each ligand type there are no free parameters in the analysis. Overall this reproduces ≈700 mV of the 800 mV found experimentally [Fig. 1(a)]. This is the first attempt to use a single method to calculate such a large range of heme E_ms. All atomic force field parameters used here are the same as used for MCCE calculations of pK_as in proteins (Song Y, Mao J, Gunner MR, in preparation).

Despite the good agreement between calculation and experiment (see Fig. 1), the His-Met *c* type E_ms are systematically lower than the experimental values [Fig. 1(a)]. If the $E_{m,calc}$ for each of these 24 proteins is shifted up by 160 mV, the slope matching the experimental and calculated values significantly increases to 0.969 with an R^2 of 0.931 [Table I, Fig. 1(b)]. With the correction, 65% of the hemes have an absolute error smaller than 60 mV, equivalent to an error of 1 pH unit (1.36 kcal/mol) in a calculation of a group pK_a and 92% are within 120 mV. This can be compared with the most recent version of MCCE analysis of the pK_as of 320 amino acids in 38 proteins where 79% of the residues have errors smaller than 1 pH unit and 97% errors smaller than 2 pH units (Song *et al.* in preparation). However, the calculation of heme electrochemistry may represent a more difficult problem because the heme is generally well buried in the protein. In contrast, the large majority of amino acids used in pK_a benchmark studies are on the protein surface where they are perturbed little by the protein.[103]

There are several possible sources of the systematic shift of the His-Met hemes. $E_{m,sol}$ influence all hemes of the same type in the same way. The $E_{m,sol}$ used here are the same as applied in earlier MCCE analysis of heme electrochemistry.[22,61] $E_{m,sol}$ for the bis-His and aquo-His hemes are taken from measurements on microperoxidases. The $E_{m,sol}$ of −15 mV for His-Met hemes is derived from the E_m shift found by mutating one His ligand to a Met in cyt *c*[69,104], in cyt c_{551}[70] and in cyt c_3.[105] The $E_{m,sol}$ for His-Met microperoxidase is −70 mV.[68] Using this value would lower the $E_{m,calc}$ by 55 mV, increasing the needed offset.

Another term that is used for all calculations on a given type of heme is the reference reaction field energy $\Delta G_{rxn,sol}$ (Table II). This provides the maximal stabilization of the heme ligand complex when it is immersed in water. A larger difference between the reaction field energy of oxidized and reduced heme allows greater positive shifts of the E_m as the heme is buried. The default $E_{m,calc}$ groups the heme and its axial ligands, with standard PARSE charges, together as a heme complex using the metal centered charges. However, in earlier calculation from this laboratory the ligands carried no charge.[22] Despite the identical shape and net charge on the heme complex, the distribution of atomic charges produces a large change in the solution reaction field energy, especially for the neutral reduced heme. In addition, the amino acid axial ligand charges produce a significant difference between the $\Delta G_{rxn,sol}$ for the bis-His and His-Met hemes. Making the solution reaction field energy less negative will shift the $E_{m,calc}$ to more negative values, because there can be a smaller penalty for oxidation of a buried heme. However, this difference again tends to lower the bis-His hemes more than the His-Met hemes so does not explain the result that the His-Met hemes are systematically too low.

Table II
Reference Reaction Field Energy (meV) Using Different Charge Sets Calculated with $\varepsilon_{in} = 4$, $\varepsilon_{out} = 80$

Heme type	Ligand type	Charge set	$G_{rxn,sol,ox}$	$G_{rxn,sol,red}$	$\Delta G_{rxn,sol}$
c	bis-His	Metal Centered	**−511**	**−260**	**−251**
		ESP[a]	−439	−204	−235
		NBO[b]	−574	−435	−139
	His-Met	Metal Centered	**−468**	**−136**	**−332**
		Quantum[c]	−478	−126	−352
b	bis-His	Metal Centered	**−510**	**−232**	**−278**
	His-Met	Metal Centered	**−473**	**−124**	**−349**
Mao et al[d]		Metal Centered	−430	−20	−410

Charges derived from Jaguar calculations using
[a]ESP: electrostatic surface potential method.
[b]NBO: natural bond orbital theory.
[c]Charges obtained with Gaussian from Autenrieth F and coworkers.[76]
[d]Reference reaction field energy used in Mao J and coworkers[22] for both bis-His and His-Met ligands.
Numbers in bold are used as default in calculation.

As $\Delta G_{rxn,sol}$ is quite sensitive to the atomic charge distribution and radii used, it would be helpful to have an experimental system to use as a model. Formally, the $\Delta G_{rxn,sol}$ would be measured by the free energy of transfer of the oxidized and reduced heme ligand complexes from water into a solvent with a dielectric constant of 4.[31] Alternately, the difference in the transfer energy of oxidized and reduced hemes can be determined from the E_m shift of the heme measured in the two solvents.[49] E_m shifts have been measured for heme in a dendritic microenvironment in water ($\varepsilon \sim 80$), MeCN ($\varepsilon \sim 40$) and CH_2Cl_2 ($\varepsilon \sim 10$).[106] This system shows increasing heme E_ms when the dendrite shell increased or when the solvent dielectric constant decreased as expected from a continuum electrostatic analysis. The smallest model system is viewed as most similar to the microperoxidases used here as the models for $E_{m,sol}$. The measured E_m is −210 mV in CH_2Cl_2, 80 mV higher than in water. The calculated change in $\Delta G_{rxn,sol}$ moving from $\varepsilon = 4$ to $\varepsilon = 80$ was compared with the transfer from $\varepsilon = 4$ to $\varepsilon = 10$. With the charge distribution on the heme-ligand complex used here, the $\Delta\Delta G_{rxn,sol}$ is 96 meV for *b*-type hemes and 80 meV for *c*-type hemes, in agreement with the dendritic model system measurements. In contrast, the charge distribution used previously with no charges on the ligands gives a much larger $\Delta\Delta G_{rxn,sol}$ of 200 mV. Thus, the current charge distribution yields more reasonable solution reaction field energies. However, the experimental

model system does not provide any information about possible differences between bis-His and His-Met hemes.

Another possible cause of the $E_{m,calc}$ for His-Met *c*-type hemes being lower than $E_{m,expt}$ is there that there is an error in the calculated ionization state of the propionates. The His-Met c-type proteins have the largest calculated $\Delta G_{res,prop}$ which lowers $E_{m,calc}$ by 80 mV, on average, more than they do in the bis-His *c*-type hemes. The calculated net charge on the two acids is often between −1 and −2. If the calculated pK_as were too low and the acids too ionized this will lower the E_ms.

The sensitivity to the propionic acid ionization can be seen in the comparison of the results of calculations on each structure in an ensemble of 40 NMR structures of reduced horse heart cytochrome *c* (pdb 2GIW, $E_{m,expt}$ 260 mV[90]). The calculated E_ms range from −14 mV to 255 mV with an average of 107 mV. This averaged value is close to the $E_{m,calc}$ obtained starting with a crystal structure. Comparing the NMR structures with the lowest and the highest calculated E_m, shows that the structure with the $E_{m,calc}$ of −14 mV has one propionate fully and the other 72% deprotonated at the midpoint of the titration. Meanwhile, the structure with an $E_{m,calc}$ of 255 meV only has one propionate ionized. This difference contributes 80 mV to the difference in $E_{m,calc}$. There is also a ≈200 meV difference in the interaction with the backbone dipoles, with the backbone of the Met80 ligand contributing 70 meV to the difference. The MCCE method can sample different propionic acid conformations, reducing the differences between different starting structural models.[38] However, differences between backbone conformations are not sampled in the calculations. This degree of difference found for an ensemble of NMR structures is not unusual in MCCE. However, the averaged pK_a[38,61] or E_ms[22] are generally similar to those found for X-ray crystal structures. The results from each structure in the ensemble often provide interesting information about how changes in conformation can affect the result electrochemistry.

The shifts in $E_{m,calc}$ with ionization of the propionic acids can also be seen in the lowest potential His-Met *c*-type hemes, both in *Rps. viridis* reaction centers ($E_{m,extp}$ −60 mV[100]) and in cyt c_{553} of *B. pasteurii* ($E_{m,expt}$ 60 mV[107]). In both the cases, the propionic acids are partially protonated. In cyt c_{553}, the A ring propionic acid is trapped at the protein surface and so only 20% ionized when the heme is fully reduced. The shifts in $E_{m,calc}$ obtained when both propionic acids on these hemes are fixed in their ionized form are shown in Figure 1(b). The $E_{m,calc}$ is now ∼90 mV lower than before and reducing the absolute error to ∼90 mV.

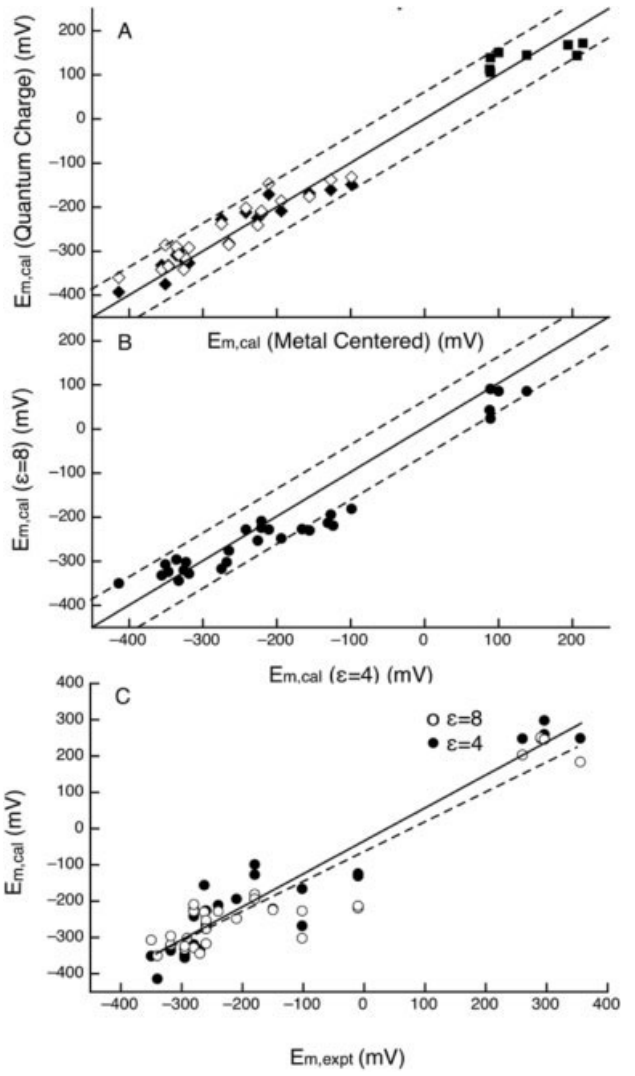

Figure 4

MCCE Calculated E_ms with different charge distribution and dielectric constants. (**a**) (■) Calculated E_ms of His-Met hemes using quantum charge set from Autenrieth F and coworkers[76] vs. metal centered charge set. Calculated E_ms of bis-His hemes using (◆) ESP and (◇) NBO charge sets vs. metal centered charge set. (**b**) (●) Calculated E_ms of selected proteins in $\varepsilon = 8$ vs. $\varepsilon = 4$. Two dashed lines are ±60 mV error lines. (**c**) Calculated E_ms using both $\varepsilon = 8$ and $\varepsilon = 4$ vs. experimental E_ms. Here, a +160 mV offset is added to all calculated His-Met c hemes for better comparison with the experimental data (See Fig. 1). The dashed line and dark line are the best-fit linear regression for calculated E_ms with $\varepsilon = 8$ (slope 0.84, R^2 0.89) and $\varepsilon = 4$ (slope 0.92, R^2 0.92), respectively.

Charge set

The sensitivity of the calculations to the heme-ligand complex charge distribution was tested [Fig. 4(a)]. The same reference reaction field energy calculated with the metal centered charge set was used for each ligand type.

Three charge sets for the bis-His hemes include the metal centered default set and ESP and NBO charges, which were derived from Jaguar calculation (Zhang J, Gunner MR, in preparation). The difference in calculated E_ms between the metal-centered charge set and the two

quantum charge sets are less than 65 mV, with both providing similar agreement with the measured data. The loss in reaction field energy ($\Delta\Delta G_{rxn}$) and backbone interactions (ΔG_{pol}) are rather similar with the different heme partial charges. The ionization states of the propionates shift very little. No significant conformation or ionization state changes in the protein were observed.

For His-Met hemes, the metal-centered charge set was compared with those obtained by previously published Gaussian calculation.[76] Small changes, which are no more than 62 mV in the calculated E_ms, were seen. The energy terms in MCCE calculation were quite constant between the two charge sets. Small variations in residue ionization states were seen. Nevertheless, its affect on the final redox midpoint potentials is small.

The influence of charge set on $E_{m,calc}$ used one value of $\Delta G_{rxn.sol}$. $\Delta G_{rxn,sol}$ is dependent on the charge distribution on the heme-ligand complex (Table II). However, except for the NBO charge set, the difference in $\Delta G_{rxn,sol}$ between charge sets for each ligand type is less than 20 meV. The NBO charge gives a reference reaction field energy ~100 meV lower than the other two, which would lower the $E_{m,calc}$ of all hemes by that much. This would tend to lower the absolute $E_{m,calc}$ but not the relative E_m for a given heme type.

Dielectric constant (ε)

The value for the dielectric constant of the protein remains one of the most contentious issues for the continuum electrostatics methodology.[37,43,108–110] MCCE calculation was carried out using both a dielectric constant of 4 and 8 on a selected group of proteins (see Fig. 4) with the default metal centered charges. $\Delta G_{rxn,sol}$ was calculated with the same ε_{in} as the protein. Of the 29 hemes selected in the calculation, five have their $E_{m,calc}$ shifted by more than 65 mV. Bovine cytochrome b_5 (pdb: 1CYO) changes by 95 mV. Here $\Delta G_{res,prot}$ change by ~13 meV. The heme loses ~50 meV less reaction field energy in $\varepsilon = 8$ than in $\varepsilon = 4$ but it interacts 60 meV more favorably with the backbone dipoles. As a result, the heme oxidation is favored by ~110 meV more in $\varepsilon = 8$ than in $\varepsilon = 4$ lowering the $E_{m,calc}$.

The change in dielectric constant shows the balance between reaction field energy and pairwise interactions. Thus, calculations with $\varepsilon = 4$ always have a more significant loss in reaction field energy than with $\varepsilon = 8$, raising the $E_{m,calc}$. The individual pairwise interactions will have a larger absolute value in the lower dielectric constant, which can lower or raise the $E_{m,calc}$ depending on the sign of a charged group or orientation of a dipole. In the larger high potential His-Met *c*-type hemes, the calculated $\Delta\Delta G_{rxn}$s with $\varepsilon = 4$ are more unfavorable by 42 to 89 meV. Although in the small, low potential bis-His *c*-type heme proteins, $E_{m,cal}$ shifts only by −2 to 36 meV. The backbone interaction which tend to raise the $E_{m,calc}$ in the higher potential hemes do so by a smaller amount with the higher dielectric constant. In the small proteins where this term is small in $\varepsilon = 4$, relatively similar backbone interactions are seen with $\varepsilon = 8$. In Figure 4(c), the calculated E_ms both using $\varepsilon = 8$ and $\varepsilon = 4$ were compared with the measured data. Best-fit linear regression lines show that the results with $\varepsilon = 4$ have a slope of 0.92 ($R^2 = 0.92$), whereas with $\varepsilon = 8$ the slope is 0.84 ($R^2 = 0.89$). Thus, overall calculations with $\varepsilon = 8$ underestimate the protein contribution to the heme E_ms.

CONCLUSIONS

It is a long-standing challenge to demonstrate how proteins modify the *in situ* properties of bound substrates and cofactors. The enormous range of heme E_ms in proteins allows us to test the hypothesis that the E_m differences in individual proteins arise predominately from the difference in the electrostatic interactions of the cofactor with the protein and the surrounding solvent. Here with only one free parameter, $E_{m,sol}$ taken from experiments,[68–70] the calculations are shown to account for ≈73% of the measured change in E_ms (Fig. 1, Table I). Thus, a good fraction of the observed range of heme E_ms in proteins can be assigned to perturbation of the reaction by changing the heme ligand and by the nonbonded electrostatic interactions with the protein and solvent, which are captured in the MCCE calculations. The free energy changes that arise from proton release upon heme oxidation are included in this analysis. The errors are not uniformly distributed. Rather the his-met *c*-type hemes are calculated to be too easily oxidized in their protein environment. A number of possible errors and uncertainties are considered here without satisfactorily identifying the source of the problem. Nevertheless, raising this group of E_ms with a 160 mV offset produces calculated results with a slope of 0.97 with an R^2 of 0.93 comparing calculated and experimental E_ms. With this correction, 65% of the E_ms have errors of <1.4 kcal/mol and only 7% having errors >2.8 kcal/mol. The 800 mV span studied here represents the largest range of E_ms calculated using a single method. The results provide a better understanding of heme electrochemistry in proteins and may provide rules to help in engineering heme proteins with desired properties.

Given the success of the analysis in calculating the E_ms, it becomes possible to ask what factors are most important for modulating the *in situ* electrochemistry. The interactions between heme and protein are divided into the loss of heme solvation energy ($\Delta\Delta G_{rxn}$), and pairwise interactions of the heme with the covalently attached propionic acids ($\Delta G_{res,prop}$) and the sidechains ($\Delta G_{res,prot}$) and backbone of the protein (ΔG_{pol}). Each of these energy terms is quite different in the different proteins. However, each alone is poorly correlated with the E_m. It has long been suggested that the loss of solvation

energy, which raises all E_ms would be the dominant factory in tuning the *in situ* electrochemistry.[79–81] Although the $\Delta\Delta G_{rxn}$, which is the continuum electrostatics measure of the solvation energy has the best correlation with the measured E_m, the R^2 is only 0.5 and the slope is 0.2. This indicates that no more than 20% of the E_m range can be assigned to changes in solvation energy. Proteins can also tune their E_ms by local differences in the backbone structure, by the distribution of nearby sidechains, by the ionization state and solvent exposure of their propionic acids and by the exposure of the heme itself to water. Overall this analysis shows that different proteins use a different mixture of forces to regulate its heme E_m.

ACKNOWLEDGMENTS

We thank Dr. Ronald Koder, Dr. Jessica Norman, and Dr Yifan Song for their helpful discussion and for carefully reading the manuscripts.

REFERENCES

1. Dutton PL. Redox potentiometry: determination of midpoint potentials of oxidation-reduction components of biological electron-transfer systems. Methods Enzymol 1978;54:411–435.
2. Wilson GS. Determination of oxidation-reduction potentials. Methods Enzymol 1978;54:396–410.
3. Chapman SK, Daff S, Munro AW. Heme: the most versatile redox centre in biology? Metal Sites Proteins Models 1997;88:39–70.
4. Pettigrew GW, Moore GR. Cytochromes c: biological aspects. In: Rich A, editor. Berlin: Springer-Verlag; 1987.
5. Guengerich FP, Miller GP, Hanna IH, Martin MV, Leger S, Black C, Chauret N, Silva JM, Trimble LA, Yergey JA, Nicoll-Griffith DA. Diversity in the oxidation of substrates by cytochrome P450 2D6: lack of an obligatory role of aspartate 301-substrate electrostatic bonding. Biochemistry 2002;41:11025–11034.
6. Antonin E, Brunori M. Hemoglobin and myoglobin in their reactions with ligands. Amsterdam: North-Holland; 1971.
7. Harrison P, Huehns ER. Proteins of iron metabolism. Nature 1979;279:476–477.
8. Rodgers KR. Heme-based sensors in biological systems. Curr Opin Chem Biol 1999;3:158–167.
9. Chan MK. Recent advances in heme-protein sensors. Curr Opin Struct Biol 2001;5:216–222.
10. Liu X, Kim CN, Yang J, Jemmerson R, Wang X. Induction of apoptotic program in cell-free extracts: requirement for dATP and cytochrome c. Cell 1996;86:147–157.
11. Wilson JD, Giesselman BR, Mitra S, Foster TH. Lysosome-damage-induced scattering changes coincide with release of cytochrome c. Opt Lett 2007;32:2517–2519.
12. Discher BM, Koder RL, Moser CC, Dutton PL. Hydrophilic to amphiphilic design in redox protein maquettes. Curr Opin Chem Biol 2003;7:741–748.
13. Hecht MH, Das A, Go A, Bradley LH, Wei Y. De novo proteins from designed combinatorial libraries. Protein Sci 2004;13:1711–1723.
14. Haehnel W. Chemical synthesis of TASP arrays and their application in protein design. Mol Divers 2004;8:219–229.
15. Izadi N, Henry Y, Haladjian J, Goldberg ME, Wandersman C, Delepierre M, Lecroisey A. Purification and characterization of an extracellular heme-binding protein. Has A, involved in heme iron acquisition. Biochemistry 1997;36:7050–7057.
16. Arciero DM, Hooper AB. A di-heme cytochrome c peroxidase from nitrosomonas europaea catalytically active in both the oxidized and half-reduced states. J Biol Chem 1994;269:11878–11886.
17. Reedy CJ, Gibney BR. Heme protein assemblies. Chem Rev 2004;104:617–649.
18. Gunner MR, Honig B. Electrostatic control of midpoint potentials in the cytochrome subunit of the *Rhodopseudomonas viridis* reaction center. Proc Natl Acad Sci USA 1991;88:9151–9155.
19. Ullmann GM. The coupling of protonation and reduction in proteins with multiple redox centers: theory, computational method, and application in cytochrome c_3. J Phys Chem B 2000;104:6293–6301.
20. Teixeira VH, Soares CM, Baptista AM. Studies of the reduction and protonation behavior of tetraheme cytochromes using atomic detail. J Biol Inorg Chem 2002;7:200–216.
21. Ishikita H, Loll B, Biesiadka J, Saenger W, Knapp EW. Redox potentials of chlorophylls in photosystem II reaction center. Biochemistry 2005;44:4118–4124.
22. Mao J, Hauser K, Gunner MR. How cytochromes with different folds control heme redox potentials. Biochemistry 2003;42:9829–9840.
23. Churg AK, Weiss RM, Warshel A, Takano T. On the action of cytochrome c: correlating geometry changes upon oxidation with activation energies of electron transfer. J Phys Chem 1983;87:1683–1694.
24. Sham YY, Chu ZT, Warshel A. Consistent calculations of pK_a's of ionizable residues in proteins: semi-microscopic and microscopic approaches. J Phys Chem 1997;101:4458–4472.
25. Oliveira AS, Teixeira VH, Baptista AM, Soares CM. Reorganization and conformational changes in the reduction of tetraheme cytochromes. Biophys J 2005;89:3919–3930.
26. Bhattacharyya S, Stankovich MT, Truhlar DG, Gao J. Combined quantum mechanical and molecular mechanical simulations of one- and two-electron reduction potentials of flavin cofactor in water, medium-chain acyl-CoA dehydrogenase, and cholesterol oxidase. J Phys Chem A 2007;111:5729–5742.
27. Voigt P, Knapp EW. Tuning heme redox potentials in the cytochrome c subunit of photosynthetic reaction centers. J Biol Chem 2003;278:51993–52001.
28. Hauser K, Mao J, Gunner MR. pH dependence of heme electrochemistry in cytochromes investigated by multiconformation continuum electrostatic calculations. Biopolymers 2004;74:51–54.
29. Rogers NK, Moore GR, Sternberg MJE. Electrostatic interactions in globular proteins: calculation of the pH dependence of the redox potential of cytochrome c_{551}. J Mol Biol 1985;182:613–616.
30. Gunner MR, Alexov E. A pragmatic approach to structure based calculation of coupled proton and electron transfer in proteins. Biochim Biophys Acta 2000;1458:63–87.
31. Gunner MR, Mao J, Song Y, Kim J. Factors influencing energetics of electron and proton transfers in proteins. What can be learned from calculations. Biochim Biophys Acta 2006;1757:942–968.
32. Bashford D. Macroscopic electrostatic models for protonation states in proteins. Front Biosci 2004;9:1082–1099.
33. Beroza P, Case DA. Calculations of proton-binding thermodynamics in proteins. Method Enzymol 1998;295:170–189.
34. Ullmann GM, Knapp EW. Electrostatic models for computing protonation and redox equilibria in proteins. Eur Biophys J 1999;28:533–551.
35. Neves-Petersen MT, Petersen SB. Protein electrostatics: a review of the equations and methods used to model electrostatic equations in biomolecules–applications in biotechnology. Biotechnol Annu Rev 2003;9:315–395.
36. Alexov EG, Gunner MR. Incorporating protein conformational flexibility into the calculation of pH-dependent protein properties. Biophys J 1997;72:2075–2093.
37. Warshel A, Papazyan A. Electrostatic effects in macromolecules: fundamental concepts and practical modeling. Curr Opin Struct Biol 1998;8:211–217.

38. Georgescu RE, Alexov EG, Gunner MR. Combining conformational flexibility and continuum electrostatics for calculating pK_as in proteins. Biophys J 2002;83:1731–1748.
39. Toseland CP, McSparron H, Davies MN, Flower DR. PPD v1.0–an integrated, web-accessible database of experimentally determined protein pKa values. Nucleic Acids Res 2006;34 (Database issue):D199–D203.
40. Song Y, Gunner MR. Comparison of bacteriorhodopsin and halorhodopsin by MCCE reveals a possible new chloride binding site in halorhodopsin. Biophys J 2004;86:611a–611a.
41. Paddock ML, Rongey SH, Feher G, Okamura MY. Pathway of proton transfer in bacterial reaction centers: replacement of glutamic acid 212 in the L subunit by glutamine inhibits quinone (secondary acceptor) turnover. Proc Natl Acad Sci USA 1989;86: 6602–6606.
42. Kassner RJ. Effects of nonpolar environments on the redox potentials of heme complexes. Proc Natl Acad Sci USA 1972;69:2263–2267.
43. Warshel A, Russell ST. Calculations of electrostatic interactions in biological systems and in solutions. Q Rev Biophys 1984;17:283–422.
44. Kadish KM. Electrochemistry of metalloporphyrins in nonaqueous media. Prog Inorg Chem 1986;34:435–605.
45. Nicholls A, Honig B. A rapid finite difference algorithm utilizing successive over-relaxation to solve the Poisson-Boltzmann equation. J Comp Chem 1991;12:435–445.
46. Bashford D, Case DA. Generalized Born models of macromolecular solvation effects. Annu Rev Phys Chem 2000;51:129–152.
47. Onufriev A, Bashford D, Case DA. Modification of the generalized Born model suitable for macromolecules. J Phys Chem B 2000;104:3712–3720.
48. Velin Z, Spassov HL, Gerwert K, Bashford D. pKa calculations suggest of an excess proton in a hydrogen-bonded water network in bacteriorhodopsin. J Mol Biol 2001;312:203–219.
49. Rabenstein B, Ullmann GM, Knapp E-W. Energetics of electron-transfer and protonation reactions of the quinones in the photosynthetic reaction center of *Rhodopseudonas viridis*. Biochemistry 1998;37:2488–2495.
50. Antosiewicz J, McCammon JA, Gilson MK. The determinants of pK_as in proteins. Biochemistry 1996;35:7819–7833.
51. Sandberg L, Edholm O. A fast and simple method to calculate protonation states in proteins. Proteins 1999;36:474–483.
52. Sharp K, Jean-Charles A, Honig B. A local dielectric constant model for solvation free energies which accounts for solute polarizability. J Phys Chem 1992;96:3822–3828.
53. Teixeira VH, Cunha CA, Machuqueiro M, Oliveira ASF, Victor BL, Soares CM, Baptista AM. On the use of different dielectric constants for computing individual and pairwise terms in Poisson-Boltzmann studies of protein ionization equilibrium. J Phys Chem B 2005;109:14691–14706.
54. Song Y, Mao J, Gunner MR. Calculation of proton transfers in bacteriorhodopsin bR and M intermediates. Biochemistry 2003; 42:9875–9888.
55. Zhu Z, Gunner MR. Energetics of quinone-dependent electron and proton transfers in *Rhodobacter sphaeroides* photosynthetic reaction centers. Biochemistry 2005;44:82–96.
56. Haas AH, Lancaster CR. Calculated coupling of transmembrane electron and proton transfer in dihemic quinol: fumarate reductase. Biophys J 2004;87:4298–4315.
57. Tang CL, Alexov E, Pyle AM, Honig B. Calculation of pKas in RNA: on the structural origins and functional roles of protonated nucleotides. J Mol Biol 2007;366:1475–1496.
58. Verissimo AF, Sousa FL, Baptista AM, Teixeira M, Pereira MM. Thermodynamic redox behavior of the heme centers of cbb(3) heme-copper oxygen reductase from bradyrhizobium japonicum. Biochemistry 2007;46:13245–13253.
59. Fufezan C, Zhang J, Gunner MR. Ligand preference and orientation in b- and c-type heme-binding proteins. Proteins 2008;73: 690–704.
60. Berman HM, Westbrook J, Feng Z, Gilliland G, Bhat TN, Weissig H, Shindyalov IN, Bourne PE. The protein data bank. Nucleic Acid Res 2000;28:235–242.
61. Song Y, Mao J, Gunner MR. Electrostatic environment of hemes in proteins: pK_as of hydroxyl ligands. Biochemistry 2006;45:7949–7958.
62. Song Y, Michonova-Alexova E, Gunner MR. Calculated proton uptake on anaerobic reduction of cytochrome c oxidase: is the reaction electroneutral? Biochemistry 2006;45:7959–7975.
63. Alexov EG, Gunner MR. Calculated protein and proton motions coupled to electron transfer: electron transfer from Q_A^- to Q_B in bacterial photosynthetic reaction centers. Biochemistry 1999;38: 8253–8270.
64. Sitkoff D, Sharp KA, Honig B. Accurate calculation of hydration free-energies using macroscopic solvent models. J Phys Chem 1994;98:1978–1988.
65. Gilson MK, Honig B. Calculation of the total electrostatic energy of a macromolecular system: solvation energies, binding energies, and conformational analysis. Proteins 1988;4:7–18.
66. Pearlman DA, Case DA, Caldwell JW, Ross WS, Cheatham TE, III, DeBolt S, Ferguson D, Seibel G, Kollman P. AMBER a package of computer programs for applying molecular mechanics, normal mode analysis, molecular dynamics and free energy calculations to simulate the structural and energetic properties of molecules. Comput Phys Commun 1995;91:1–41.
67. Kassner RJ. A theoretical model for the effects of local nonpolar heme environments on the redox potentials in cytochromes. J Am Chem Soc 1973;95:2674–2676.
68. Wilson GS. Electrochemical studies of porphyrin redox reactions as cytochromes models. Bioelectrochem Bioenerg 1974;1:172–179.
69. Raphael AL, Gray HB. Axial ligand replacement in horse heart cytochrome c by semisynthesis. Proteins 1989;6:338–340.
70. Miller GT, Zhang B, Hardman JK, Timkovich R. Converting a c-type to a b-type cytochrome: Met61 to His61 mutant of pseudomonas cytochrome c-551. Biochemistry 2000;39:9010–9017.
71. Matthew JB, Gurd FRN, Garcia-Moreno B, Flanagan MA, March KL, Shire SJ. pH-dependent processes in proteins. CRC Crit Rev Biochem 1985;18:91–197.
72. Munro OQ, Marques HM. Heme-peptide models for hemoproteins. 1. solution chemistry of *N*-acetylmicroperoxidase-8. Inorg Chem 1996;35:3752–3767.
73. Vashi PR, Marques HM. The coordination of imidazole and substituted pyridines by the hemeoctapeptide *N*-acetyl-ferromicroperoxidase-8 (Fe^{II}NAcMP8). J Inorg Biochem 2004;98:1471–1482.
74. Marques HM, Cukrowski I, Vashi PR. Co-ordination of weak field ligands by *N*-acetylmicroperoxidase-8 (NAcMP8), a ferric haem-peptide from cytochrome c, and the influence of the axial lignad on the reduction potential of complexes of NAcMP8. J Chem Soc 2000;2000:1335–1342.
75. Lide DR. CRC handbook of chemistry and physics. Boca Raton: CRC Press; 1990.
76. Autenrieth F, Tajkhorshid E, Baudry J, Luthey-Schulten Z. Classical force field parameters for the heme prosthetic group of cytochrome c. J Comput Chem 2004;25:1613–1622.
77. Jaguar, version 7.0: Schrödinger, LLC, New York, NY; 2007.
78. Datta S, Mori Y, Takagi K, Kawaguchi K, Chen ZW, Okajima T, Kuroda S, Ikeda T, Kano K, Tanizawa K, Mathews FS. Structure of a quinohemoprotein amine dehydrogenase with an uncommon redox cofactor and highly unusual crosslinking. Proc Natl Acad Sci USA 2001;98:14268–14273.
79. Stellwagen E. Haem exposure as the determinate of oxidation-reduction potential of haem proteins. Nature 1978;275:73–74.
80. Tezcan FA, Winkler JR, Gray HB. Effects of ligation and folding on reduction potentials of heme proteins. J Am Chem Soc 1998;120:13383–13388.
81. Fantuzzi A, Sadeghi S, Valentti F, Rossi GL, Gilardi G. Tuning the reduction potential of engineered cytochrome c-553. Biochemistry 2002;41:8718–8724.

82. Gunner MR, Nicholls A, Honig B. Electrostatic potentials in Rhodopseudomonas viridis reaction center: implications for the driving force and directionality of electron transfer. J Phys Chem 1996;100:4277–4291.
83. Harada E, Kumagai J, Ozawa K, Imabayashi S, Tsapin AS, Nealson KH, Meyer TE, Cusanovich MA, Akutsu H. A directional electron transfer regulator based on heme-chain architecture in the small tetraheme cytochrome c from Shewanella oneidensis. FEBS Lett 2002;532:333–337.
84. Kraus DW, Wittenberg JB. Hemoglobins of the *Lucina pectinata*/bacteria symbiosis. I. Molecular properties, kinetics and equilibria of reactions with ligands. J Biol Chem 1990;265:16043–16053.
85. Gunner MR, Saleh MA, Cross E, ud-Doula A, Wise M. Backbone dipoles generate positive potentials in all proteins: origins and implications of the effect. Biophys J 2000;78:1126–1144.
86. Roncel M, Boussac A, Zurita JL, Bottin H, Sugiura M, Kirilovsky D, Ortega JM. Redox properties of the photosystem II cytochromes b559 and c550 in the cyanobacterium Thermosynechococcus elongatus. J Biol Inorg Chem 2003;8:206–216.
87. Drepper F, Dorlet P, Mathis P. Cross-linked electron transfer complex between cytochrome c2 and the photosynthetic reaction center of Rhodobacter sphaeroides. Biochemistry 1997;36:1418–1427.
88. Xue L, Wang Y, Xie Y, Yao P, Wang W, Qian W, Huang Z. Effect of mutation at valine 61 on the three-dimensional structure, stability, and redox potential of cytochrome b5. Biochemistry 1999;38:11961–11972.
89. Moore GR. Control of redox properties of cytochrome c by special electrostatic interactions. FEBS Lett 1983;161:171–175.
90. Moore GR. Haemoproteins. In: Bendall DS, editor. Protein electron transfer. Cambridge: Bios; 1996. pp 189–216.
91. Malarte G, Leroy G, Lojou E, Abergel C, Bruschi M, Giudici-Orticoni MT. Insight into molecular stability and physiological properties of the diheme cytochrome CYC41 from the acidophilic bacterium Acidithiobacillus ferrooxidans. Biochemistry 2005;44:6471–6481.
92. Gayda JP, Benosman H, Bertrand P, More C, Asso M. EPR determination of interaction redox potentials in a multiheme cytochrome: cytochrome c_3 from *Desulfovibrio desulfuricans* Norway. Eur J Biochem 1988;177:199–206.
93. Rivera M, Seetharaman R, Girdhar D, Wirtz M, Zhang X, Wang X, White S. The reduction potential of cytochrome b5 is modulated by its exposed heme edge. Biochemistry 1998;37:1485–1494.
94. Springs SL, Bass SE, Bowman G, Nodelman I, Schutt CE, McLendon GL. A multigeneration analysis of cytochrome b_{562} redox variants: evolutionary strategies for modulating redox potential revealed using a library approach. Biochemistry 2002;41:4321–4328.
95. Tomlinson EJ, Ferguson SJ. Conversion of a c type cytochrome to a b type that spontaneously forms in vitro from apo protein and heme: implications for c type cytochrome biogenesis and folding. Proc Natl Acad Sci USA 2000;97:5156–5160.
96. Zhuang J, Amoroso JH, Kinloch R, Dawson JH, Baldwin MJ, Gibney BR. Evaluation of electron-withdrawing group effects on heme binding in designed proteins: implications for heme a in cytochrome c oxidase. Inorg Chem 2006;45:4685–4694.
97. Springs SL, Bass SE, McLendon GL. Cytochrome b562 variants: a library for examing redox potential evolution. Biochemistry 2000; 39:6075–6082.
98. Weiland TR, Kundu S, Trent JT, III, Hoy JA, Hargrove MS. Bishistidyl hexacoordination in hemoglobins facilitates heme reduction kinetics. J Am Chem Soc 2004;126:11930–11935.
99. Gray HB, Winkler JR. Electron tunneling through proteins. Q Rev Biophys 2003;36:341–372.
100. Dracheva SM, Drachev LA, Konstantinov AA, Semenov AY, Skulachev VP, Arutjunjan AM, Shuvalov VA, Zaberezhnaya SM. Electrogenic steps in the redox reactions catalyzed by photosynthetic reaction-centre complex from *Rhodopseudomonas viridis*. Eur J Biochem 1988;171:253–264.
101. Zhen Y, Schmidt B, Kang UG, Antholine W, Ferguson-Miller S. Mutants of the CuA site in cytochrome c oxidase of Rhodobacter sphaeroides: I. Spectral and functional properties. Biochemistry 2002;41:2288–2297.
102. Fujieda N, Mori M, Kano K, Ikeda T. Spectroelectrochemical evaluation of redox potentials of cysteine tryptophylquinone and two hemes c in quinohemoprotein amine dehydrogenase from Paracoccus denitrificans. Biochemistry 2002;41:13736–13743.
103. Davies MN, Toseland CP, Moss DS, Flower DR. Benchmarking pK(a) prediction. BMC Biochem 2006;7:18.
104. Wallace CJA, Clark-Lewis I. Functional role of heme ligation in cytochrome c: effects of replacement of methionine 80 with natural and non-natural residues by semisynthesis. J Biol Chem 1992;1992:3852–3861.
105. Mus-Veteau I, Dolla A, Guerlesquin F, Payan F, Czjzek M, Haser R, Bianco P, Haladjian J, Rapp-Giles BJ, Wall JD. Site-directed mutagenesis of tetraheme cytochrome c3. Modification of oxidoreduction potentials after heme axial ligand replacement. J Biol Chem 1992;267:16851–16858.
106. Diederich F, Felber B. Supramolecular chemistry of dendrimers with functional cores. Proc Natl Acad Sci USA 2002;99:4778–4781.
107. Stefano Benini MB, Stefano C, Alexander D, Matteo L. Modulation of Bacillus pasteurii cytochrome c553 reduction potential by structural and solution parameters. JBIC 1998;3:371–382.
108. Gilson MK, Honig BH. The dielectric constant of a folded protein. Biopolymers 1986;25:2097–2119.
109. Harvey S. Treatment of electrostatic effects in macromolecular modeling. Proteins 1989;5:78–92.
110. Sham YY, Muegge I, Warshel A. The effect of protein relaxation on charge-charge interactions and dielectric constant of proteins. Biophys J 1998;74:1744–1753.
111. Wirtz M, Oganesyan V, Zhang X, Studer J, Rivera M. Modulation of redox potential in electron transfer proteins: effects of complex formation on the active site microenvironment of cytochrome b_5. Faraday Discuss 2000;116:221–234.
112. Northup SH. Computer modelling of protein-protein interactions. In: Bendall DS, editor. Protein electron transfer. Cambridge: Bios; 1996. pp 69–98.
113. Meyer TE, Watkins JA, Przysiecki CT, Tollin G, Cusanovich MA. Electron-transfer reactions of photoreduced flavin analogues with c-type cytochromes: quantitation of steric and electrostatic factors. Biochemistry 1984;23:4761–4767.
114. Samyn B, Fitch J, Meyer TE, Cusanovich MA, Van Beeumen JJ. Purification and primary structure analysis of two cytochrome c_2 isozymes from the purple phototrophic *bacterium Rhodospirillum centenum*. Biochim Biophys Acta 1998;1384:345–355.
115. Pettigrew GW, Bartsch RG, Meyer TE, Kamen MD. Redox potential of the photosynthetic bacterial cytochromes c_2 and the structural bases for variability. Biochim Biophys Acta 1978;503:509–523.
116. Meyer TE, Kamen MD. New perspectives on c-type cytochromes. Adv Protein Chem 1982;35:105–212.
117. Louro RO, Catarino T, Turner DL, Picarra-Pereira MA, Pacheco I, LeGall J, Xavier AV. Functional and mechanistic studies of cytochrome c_3 from *Desulfovibrio gigas*: thermodynamics of a "proton thruster." Biochemistry 1998;37:15808–15815.
118. Fan K, Akutsu H, Kyogoku Y, Niki K. Estimation of microscopic redox potentials of a tetraheme protein, cytochrome c_3 of *Desulfovibrio vulgaris*. Miyazaki F, and partial assignments of heme groups. Biochemistry 1990;29:2257–2263.
119. Turner DL, Salgeiro CA, Catarino T, Legall J, Xavier V. NMR studies of cooperativity in the teprahaem cytochrome c_3 from *Desulfovibrio vulgaris*. Eur J Biochem 1996;241:723–731.
120. Pieulle L, Haladjian J, Bonicel J, Hatchikian EC. Biochemical studies of the c-type cytochromes of the sulfate reducer *Desulfovibrio africanus*. Characterization of two tetraheme cytochromes c_3 with different specificity. Biochim Biophys Acta 1996;1273:51–61.

121. Leitch FA, Brown KR, Pettigrew GW. Complexity in the redox titration of the dihaem cytochrome c_4. Biochim Biophys Acta 1985;808:213–218.
122. Navarro JA, Hervas M, De la Cerda B, De la Rosa MA. Purification and physicochemical properties of the low-potential cytochrome C_{549} from the *cyanobacterium Synechocystis sp.* PCC 6803. Arch Biochem Biophys 1995;318:46–52.
123. Holton RW, Myers J. Water-soluble cytochromes from a blue-gree alga. II. Physicochemical properties and quantitative relationships of cytochromes C (549, 552, and 554 *Anacystis nidulans*). Biochim Biophys Acta 1967;131:375–384.
124. Lommen A, Ratsma A, Bijlsma N, Canters GW, van Wielink JE, Frank J, van Beeumen J. Isolation and characterization of cytochrome c_{550} from the methylamine-oxidizing electron-transport chain of *Thiobacillus versutus*. Eur J Biochem 1990;192:653–661.
125. Saraiva LM, Fauque G, Besson S, Moura I. Physico-chemical and spectroscopic properties of the monohemic cytochrome C_{552} from *Pseudomonas nautica* 617. Eur J Biochem 1994;224:1011–1017.
126. Terui N, Tachiiri N, Matsuo H, Hasegawa J, Uchiyama S, Kobayashi Y, Igarashi Y, Sambongi Y, Yamamoto Y. Relationship between redox function and protein stability of cytochromes c. J Am Chem Soc 2003;125:13650–13651.
127. Campos AP, Aguiar AP, Hervas M, Regalla M, Navarro JA, Ortega JM, Xavier AV, De La Rosa MA, Teixeira M. Cytochrome c_6 from *Monoraphidium braunii*. A cytochrome with an unusual heme axial coordination. Eur J Biochem 1993;216:329–341.
128. Gorman DS, Levine RP. Photosynthetic electron transport chain of *Chlamydomonas reinhardi*. V. Purification and properties of cytochrome 553 and ferredoxin. Plant Physiol 1966;41:1643–1647.
129. Cho YS, Wang QJ, Krogmann D, Whitmarsh J. Extinction coefficients and midpoint potentials of cytochrome c_6 from the *cyanobacteria Arthrospira maxima*. *Microcystis aeruginosa*, and *Synechocystis* 6803. Biochim Biophys Acta 1999;1413:92–97.
130. Dikiy A, Carpentier W, Vandenberghe I, Borsari M, Safarov N, Dikaya E, Van Beeumen J, Ciurli S. Structural basis for the molecular properties of cytochrome c_6. Biochemistry 2002;41:14689–14699.
131. Correia IJ, Paquete CM, Louro RO, Catarino T, Turner DL, Xavier AV. Thermodynamic and kinetic characterization of trihaem cytochrome c_3 from *Desulfuromonas acetoxidans*. Eur J Biochem 2002;269:5722–5730.
132. Fulop V, Ridout CJ, Greenwood C, Hajdu J. Crystal structure of the di-haem cytochrome c peroxidase from *Pseudomonas aeruginosa*. Structure 1995;3:1225–1233.
133. Santos H, Turner DL. Characterization and NMR studies of a novel cytochrome c isolated from Methylophilus methylotrophus which shows a redox-linked change of spin state. Biochim Biophys Acta 1988;954:277–286.
134. Engel WD, Schagger H, von Jagow G. Ubiquinol-cytochrome c reductase (EC 1.10.2.2). Isolation in triton X-100 by hydroxyapatite and gel chromatography. Structural and functional properties. Biochim Biophys Acta 1980;592:211–222.
135. Moody AJ, Rich PR. The effect of pH on redox titrations of Heme a in cyanide liganded cytochrome c oxidase—experimental and modeling studies. Biochim Biophys Acta 1990;1015:205–215.
136. Hellwig P, Grzybek S, Behr J, Ludwig B, Michel H, Mantele W. Electrochemical and ultraviolet/visible/infrared spectroscopic analysis of heme a and a_3 redox reactions in the cytochrome c oxidase from *Paracoccus denitrificans*: separation of heme a and a_3 contributions and assignment of vibrational modes. Biochemistry 1999;38:1685–1694.